



Deposited via The University of Sheffield.

White Rose Research Online URL for this paper:

<https://eprints.whiterose.ac.uk/id/eprint/79378/>

Monograph:

Zhang, H. and Billings, S.A. (1992) Analysing the Transfer Functions of Nonlinear Systems In the Frequency Domain. UNSPECIFIED. ACSE Research Report 445 . Department of Automatic Control and Systems Engineering

Reuse

Items deposited in White Rose Research Online are protected by copyright, with all rights reserved unless indicated otherwise. They may be downloaded and/or printed for private study, or other acts as permitted by national copyright laws. The publisher or other rights holders may allow further reproduction and re-use of the full text version. This is indicated by the licence information on the White Rose Research Online record for the item.

Takedown

If you consider content in White Rose Research Online to be in breach of UK law, please notify us by emailing eprints@whiterose.ac.uk including the URL of the record and the reason for the withdrawal request.

Analysing the Transfer Functions of Nonlinear Systems

In the Frequency Domain

H. ZHANG and S. A. BILLINGS

Department of Automatic Control & Systems Engineering

University of Sheffield

SI 4DU

UK

Research Report No.445

Jan 1992

January 29, 1992

Analysing the Transfer Functions of Nonlinear Systems In the Frequency Domain

H. ZHANG and S.A. BILLINGS

Department of Automatic Control and Systems Engineering

University of Sheffield, Sheffield S1 4DU, U.K.

Abstract:

Both continuous and discrete time transfer functions of nonlinear systems are analysed and interpreted in the frequency domain by investigating the properties and graphical representation of these functions. The contributions that some typical terms from nonlinear time domain models make to the transfer functions is illustrated to provide a better understanding of the frequency response behaviour of complex nonlinear dynamic systems.

1. Introduction

The transfer function approach of linear systems theory is an invaluable tool which provides both a simple visual representation and a clear understanding of systems behaviour and has become the cornerstone of classical control. Although it would be very desirable to have similar techniques available for nonlinear system analysis, progress in this direction has been limited both by difficulties in obtaining the transfer functions of practical systems, and by difficulties in their presentation and interpretation. By applying a recursive "probing" algorithm to NARMAX (Nonlinear Autoregressive Moving Average model with Exogenous inputs) models, it is now possible to obtain the nonlinear frequency response functions of many real systems (Kim and Powers 1988; Billings and Tsang 1989; Peyton-Jones and

Billings 1989; Billings and Peyton-Jones 1990; Tomlinson and Billings 1991) so that the analysis and application of nonlinear transfer functions become more realistic.

The transfer function approach for general nonlinear systems has two principle differences compared to the traditional linear techniques. The first is that the transfer function representation of an equivalent time-domain nonlinear system consists of a sequence of transfer functions instead of only one function in the linear case. This is a consequence of the Volterra functional polynomial which is used to define the transfer functions. The stronger the nonlinearities are, the more transfer functions are needed. But for a wide class of nonlinear systems, most of the dominant effects are contained in the first, second and third order transfer functions and these are often sufficient to characterise the system (Wiener and Spina, 1980; Vinh et al, 1987). The second difference is that each nonlinear transfer function is a multi-variate function even when the underlying system is single-input/single output. This not only increases the difficulty of analysis but also makes it very complicated to relate the transfer function to the system response characteristics to provide a physical interpretation of the effects. Indeed, the nonlinear transfer function concept was introduced in the late 1950's but very few applications were reported and little work was done on the graphical representations, which play an important role in the linear case, until very recently. Encouraged by the success in the computation and support of modern computer graphical packages and a new and efficient method of computing the transfer functions from real data, a new trend in the studies of nonlinear transfer functions has begun (Billings and Tsang, 1989; Billings and Peyton-Jones, 1990). In the present study the nonlinear transfer function is analysed by means of analytical as well as graphical methods. In section 2, the representation of a nonlinear system in both the time and transform-domain are reviewed and the transfer function concepts are clarified. The

nonlinear transfer function is then related directly to the frequency response of the system by the multi-tone input method and a meaningful interpretation is obtained. After discussing some important properties of transfer functions, the way in which nonlinear terms in the time-domain model are mapped into and affect the transfer functions are studied in section 4. Using examples it is shown how the time domain terms contribute to and induce dominant effects in the nonlinear frequency response functions. This in turn suggests how measured transfer function plots can be decomposed into the union of simple effects to provide an interpretation of the underlying systems nonlinear characteristics.

2. Representations of Nonlinear Systems in the Time- and Transform-Domain

It is well known that a nonlinear system can be described in the time domain by the input/output representation

$$y(t) = \sum_{n=1}^{\infty} y_n(t) = \sum_{n=1}^{\infty} \int_{-\infty}^{\infty} \cdots \int_{-\infty}^{\infty} h_n(\tau_1, \cdots, \tau_n) \prod_{i=1}^n u(t-\tau_i) d\tau_i \quad (1)$$

which is called the Volterra functional series. In this representation, the system output $y(t)$ is structured as a sum of the response of a possibly infinite combination of parallel subsystems, each of which is characterised by an n -th order kernel, $h_n(\tau_1, \dots, \tau_n)$, $n=1,2,\dots$. These ' n th-order outputs' are themselves defined by an extension of the familiar convolution integral of linear system theory to higher dimension

$$y_n(t) = \int_{-\infty}^{\infty} \cdots \int_{-\infty}^{\infty} h_n(\tau_1, \cdots, \tau_n) \prod_{i=1}^n u(t-\tau_i) d\tau_i \quad n > 0 \quad (2)$$

Each subsystem represented by the above homogenous functional of n th degree is called a degree- n homogenous system. In many practical applications, a finite number of homogenous subsystems will

be sufficient to represent a nonlinear system as long as the nonlinearities are not too violent.

Just as in the linear case, the n th-order kernel $h_n(\tau_1, \dots, \tau_n)$ can be called an n th-order impulse response and this characterises the n th-order homogenous subsystem in the time domain. The Laplace transform (multi-dimensional when $n > 1$) of these functions is called the n th order transfer function

$$H_n(s_1, \dots, s_n) = \int_0^{\infty} \dots \int_0^{\infty} h_n(\tau_1, \dots, \tau_n) e^{-(s_1\tau_1 + \dots + s_n\tau_n)} d\tau_1 \dots d\tau_n \quad (3)$$

Naturally it is desirable to find a similar form of input-output relationship such as $Y(s) = H(s)U(s)$ which exists in the linear case. However due to the dimensional properties there is no direct way to do this. An indirect way is adopted by amending eqn.(2) and introducing an auxiliary multidimensional time function

$$y_n(t_1, \dots, t_n) = \int_{-\infty}^{\infty} \dots \int_{-\infty}^{\infty} h_n(\tau_1, \dots, \tau_n) u(t_1 - \tau_1) \dots u(t_n - \tau_n) d\tau_i \quad n > 0 \quad (4)$$

where the real output $y_n(t)$ is recovered by the restriction,

$$y_n(t) = y_n(t_1, \dots, t_n) |_{t_1 = \dots = t_n = t} \quad (5)$$

The multidimensional Laplace transform may be applied to both sides of eqn.(4) without difficulty to yield

$$Y_n(s_1, \dots, s_n) = H_n(s_1, \dots, s_n) U(s_1) \dots U(s_n) \quad (6)$$

which reduces to the familiar linear transfer function definition for the case $n=1$.

Therefore $h_n(\tau_1, \dots, \tau_n)$ and $H_n(s_1, \dots, s_n)$ provide two equivalent representations in the time-

and transform-domain, respectively for the n th-order homogenous subsystem. Notice that both the impulse response function and the transfer function are independent of the input excitation. This is a highly desirable feature because it enables the determination of the system response for arbitrary inputs. Of these two representations we will mainly concentrate on the analysis of the transfer function since the use of the impulse response functions would involve cumbersome multiple convolution integrals.

Next it is necessary to clarify some notational confusion caused by the different transforms of Fourier, Laplace and Z. In the presentation above the transform domain representation of continuous-time systems has been presented based on the Laplace transform. Alternatively the transfer function can also be introduced by means of the Fourier transform. For a homogeneous nonlinear system of n th-degree taking the n -dimensional Fourier transform of the kernel (impulse response) we obtain

$$H_n(j\omega_1, \dots, j\omega_n) = \int_{-\infty}^{\infty} \dots \int_{-\infty}^{\infty} h_n(\tau_1, \dots, \tau_n) e^{-j(\omega_1\tau_1 + \dots + \omega_n\tau_n)} d\tau_1 \dots d\tau_n \quad (7)$$

which is also called the generalised frequency response function or system function. Notice the close link between the Fourier and Laplace transforms. It is usual for the Laplace transform to be defined as one-sided (from zero to infinity) and the Fourier transform to be defined as two-sided. If a Laplace transfer function $H_n(s_1, \dots, s_n)$ exists for $Re[s_i] \geq 0, i=1, \dots, n$, the Fourier transfer function is given by the simple relationship

$$H_n(j\omega_1, \dots, j\omega_n) = H_n(s_1, \dots, s_n)|_{s_1=j\omega_1, \dots, s_n=j\omega_n} \quad (8)$$

For a sampled-data degree- n homogeneous system the output can be calculated at regularly spaced sampling instants by means of a weighted sum of input values

$$y_n(k) = \sum_{i_1=0}^{\infty} \cdots \sum_{i_n=0}^{\infty} h_n(i_1, \dots, i_n) u(k-i_1) \dots u(k-i_n) \quad k=0,1,2,\dots \quad (9)$$

where the kernel $\{h_n(i_1, \dots, i_n)\}$ is a real sequence and equal to zero if any argument is negative (one-sided). The above equation can easily be derived by discretising the convolution integral eqn.(2) and hence is also called a 'convolution sum'. The n-dimensional Z transform of the kernel series is defined by

$$\begin{aligned} H_n(z_1, \dots, z_n) &= Z[h_n(i_1, \dots, i_n)] \\ &= \sum_{i_1=0}^{\infty} \cdots \sum_{i_n=0}^{\infty} h_n(i_1, \dots, i_n) z_1^{-i_1} \cdots z_n^{-i_n} \end{aligned} \quad (10)$$

where z_1, \dots, z_n are complex variables which are assumed to be within the region of convergence (ROC) to ensure the existence of $H_n(z_1, \dots, z_n)$. In a similar way to the linear case $H_n(\cdot)$ is called generalised pulse transfer function. There also exists a similar formulation to eqn.(6) as follows

$$Y_n(z_1, \dots, z_n) = H_n(z_1, \dots, z_n) U(z_1) \dots U(z_n) \quad (11)$$

Notice that by using delta functions the sampled form sequence $\{h_n(i_1, \dots, i_n)\}$ can be expressed as a time function as follows

$$h_n(t_1, \dots, t_n) = \sum_{i_1=0}^{\infty} \cdots \sum_{i_n=0}^{\infty} h_n(i_1 T, \dots, i_n T) \delta(t_1 - i_1 T) \dots \delta(t_n - i_n T) \quad (12)$$

where T is the sampling interval for the discrete time system. The Fourier transform is then given by substituting eqn.(12) into eqn.(7)

$$\begin{aligned} H_n(j\omega_1, \dots, j\omega_n) &= \int_{-\infty}^{\infty} \cdots \int_{-\infty}^{\infty} \sum_{i_1=0}^{\infty} \cdots \sum_{i_n=0}^{\infty} h_n(i_1 T, \dots, i_n T) \delta(\tau_1 - i_1 T) \dots \delta(\tau_n - i_n T) \\ &\quad e^{-j(\omega_1 \tau_1 + \cdots + \omega_n \tau_n)} d\tau_1 \cdots d\tau_n \end{aligned}$$

$$= \sum_{i_1=0}^{\infty} \cdots \sum_{i_n=0}^{\infty} h_n(i_1 T, \dots, i_n T) e^{-j(\omega_1 i_1 + \cdots + \omega_n i_n) T} \quad (13)$$

Therefore the (Fourier) transfer function can be viewed as $H_n(z_1, \dots, z_n)$ evaluated on the unit ball $|z_1|=|z_2|=\dots=|z_n|=1$. That is, if $H_n(z_1, \dots, z_n)$ converges on the unit ball, then

$$H_n(j\omega_1, \cdots, j\omega_n) = H_n(z_1, \cdots, z_n) \Big|_{z_1=e^{j\omega_1}, \dots, z_n=e^{j\omega_n}} \quad (14)$$

It has been shown that the Fourier representation, $H_n(j\omega_1, \cdots, j\omega_n)$, can be used for both continuous- and discrete-time nonlinear systems uniformly. Therefore in this paper we will only use the Fourier representation as the transfer function. Another advantage of the Fourier representation is the convenience for frequency response analysis. Consequently in the present paper the transform domain is actually the input frequency domain and this will be multi-dimensional for nonlinear systems. Finally notice that the principle difference between the nonlinear transfer function and multi-dimensional linear systems, although they both have multidimensional transfer functions, is that the latter have real multi-dimensional (or multi-indexed) input/output signals that are defined with integer arguments. Motivation for the study of multidimensional (usually 2D) linear systems comes mainly from the processing (or filtering) of multidimensional signals notably in image or array processing and geophysics (Fornasini and Marchesini, 1978).

3. Frequency Response Analysis using Nonlinear Transfer Functions

The main application of transfer functions is in frequency response analysis. For the case of linear systems any input frequencies pass independently through the system thus no new frequencies are produced and there is no influence or interaction between the input frequency components. However in the

response of nonlinear systems some new frequencies such as harmonics and intermodulation frequencies may appear together with effects such as gain compression/expansion and desensitisation. Even for a single frequency sinusoidal input the output of a nonlinear system may exhibit various distortions. In this section it is shown that the amplitudes and phases of various frequency components in the system output can be determined directly by the nonlinear transfer function. Before deriving the response it is useful to consider some important properties which arise for nonlinear transfer functions.

Firstly from the definition eqn.(7) an important property is immediately obvious

$$H_n(-j\omega_1, \dots, -j\omega_n) = H_n^*(j\omega_1, \dots, j\omega_n) \quad (15)$$

This is called conjugate symmetry where the asterisk is used to denote complex conjugate. This property will be useful later because negative frequencies will be encountered in the input domain.

Another interesting property follows from this observation

$$\text{Im}[H_2(j\omega, -j\omega)] = 0 \quad \text{and} \quad \text{Im}[H_4(j\omega, j\omega, -j\omega, -j\omega)] = 0 \quad (16)$$

and this causes the d.c. components in the nonlinear response because the transfer function values are real.

For any given system both $H_n(\cdot)$ and $h_n(\cdot)$ may not be unique since changing the order of argument may give different functions but will still yield the same output $y_n(t)$. There is a common practice to symmetrise the functions by summing all the asymmetric functions over all the permutations of the arguments and dividing by their number. That is,

$$H_n^{sym}(j\omega_1, \dots, j\omega_n) = \frac{1}{n!} \sum_{\substack{\text{all permutations} \\ \text{of } \omega_1 \dots \omega_n}} H_n(-j\omega_1, \dots, -j\omega_n) \quad (17)$$

In many cases the symmetric transfer function is far more convenient although it usually contains more terms than the asymmetric version. Notice that the conjugate symmetry holds for all versions of transfer function regardless of whether they are symmetric or not. All these three properties can be clearly observed in the graphical representation of the functions. For example consider a discrete-time nonlinear system

$$\text{Example 1: } y(k) = 0.84u(k-1) + 0.8y(k-1) - 0.64y(k-2) - 0.04u(k-1)u(k-3) \quad (18)$$

The symmetric second order transfer function is illustrated by the magnitude and phase angle in Fig.1(a) and (b), respectively. It is seen that the magnitude exhibits reflectional symmetry about the plane $\omega_1 = \omega_2$ and $\omega_1 = -\omega_2$, while the phase is symmetric about $\omega_1 = \omega_2$ but negative symmetric about $\omega_1 = -\omega_2$. Also it is observed that the phase is zero along $\omega_1 = -\omega_2$.

Now consider an input composed of K different sinusoids:

$$u(t) = \sum_{i=1}^K |A_i| \cos(\omega_i t + \angle A_i) = \sum_{i=1}^K \left[\frac{A_i}{2} e^{j\omega_i t} + \frac{A_i^*}{2} e^{-j\omega_i t} \right] \quad (19)$$

where A_k is a complex number to give the amplitude and phase of the k th frequency, $A_0 = 0$ and $A_{-k} = A_k^*$. Substitution of the above into eqn.(4) yields

$$\begin{aligned} y_n(t) &= \int_{-\infty}^{\infty} \cdots \int_{-\infty}^{\infty} h_n(\tau_1, \cdots, \tau_n) \prod_{i=1}^n \sum_{k=-K}^K A_k e^{j\omega_k(t-\tau_i)} d\tau_i \\ &= \sum_{k_1=-K}^K \cdots \sum_{k_n=-K}^K \int_{-\infty}^{\infty} \cdots \int_{-\infty}^{\infty} h_n(\tau_1, \cdots, \tau_n) \prod_{i=1}^n A_{k_i} e^{j\omega_{k_i}(t-\tau_i)} d\tau_i \\ &= \sum_{k_1=-K}^K \cdots \sum_{k_n=-K}^K \prod_{i=1}^n A_{k_i} e^{j\omega_{k_i} t} \int_{-\infty}^{\infty} \cdots \int_{-\infty}^{\infty} h_n(\tau_1, \cdots, \tau_n) \prod_{i=1}^n e^{-j\omega_{k_i} \tau_i} d\tau_i \end{aligned}$$

$$= \sum_{k_1=-K}^K \cdots \sum_{k_n=-K}^K \left[A_{k_1} \cdots A_{k_n} H_n(j\omega_{k_1}, \cdots, j\omega_{k_n}) \right] e^{j(\omega_{k_1} + \cdots + \omega_{k_n})t} \quad (20)$$

which together with eqn.(1) yields the frequency response of the system. Notice that in the above derivation the transfer function $H_n(\cdot)$ is not required to be symmetric although the symmetric transfer function will simplify the expression. In order to confirm the results for linear systems consider the case with $K = 2$ and $n = 1$. That is the linear component in the response to a two-tone input

$$\begin{aligned} y_1(t) &= 0.5 A_2^* H_1(-j\omega_2) e^{-j\omega_2 t} + 0.5 A_1^* H_1(-j\omega_1) e^{-j\omega_1 t} + \\ &\quad 0.5 A_1 H_1(j\omega_1) e^{j\omega_1 t} + 0.5 A_2 H_1(j\omega_2) e^{j\omega_2 t} \\ &= \text{Re}[A_2 H_1(j\omega_2) e^{-j\omega_2 t}] + \text{Re}[A_1 H_1(j\omega_1) e^{-j\omega_1 t}] \\ &= |A_2 H_1(j\omega_2)| \cos[\omega_2 t + \angle A_2 H_1(j\omega_2)] + |A_1 H_1(j\omega_1)| \cos[\omega_1 t + \angle A_1 H_1(j\omega_1)] \end{aligned}$$

which contains the two input frequencies only. This is a well known characteristic of linear systems. But in the nonlinear system response many new frequencies may be observed as well as the input frequencies and the amplitude and phase of each component will be determined by the value of the nonlinear transfer function at the corresponding points inside the input frequency domain. For example for $K = 2$ and $n = 2$ there are in total 16 terms in eqn.(20). Assuming the symmetric transfer function is used then the final response can be expressed as

$$\begin{aligned} y_2(t) &= \sqrt{|A_1 A_2 H_2(j\omega_1, j\omega_2)|} \cos[(\omega_1 + \omega_2)t + \angle A_1 A_2 H_2(j\omega_1, j\omega_2)] + \\ &\quad \sqrt{|A_1 A_2 H_2(j\omega_1, -j\omega_2)|} \cos[(\omega_1 - \omega_2)t + \angle A_1 A_2 H_2(j\omega_1, -j\omega_2)] + \\ &\quad \sqrt{0.5 |A_2 A_2 H_2(j\omega_2, j\omega_2)|} \cos[(2\omega_2)t + \angle A_2 A_2 H_2(j\omega_2, j\omega_2)] + \\ &\quad \sqrt{0.5 |A_1 A_1 H_2(j\omega_1, j\omega_1)|} \cos[(2\omega_1)t + \angle A_1 A_1 H_2(j\omega_1, j\omega_1)] + \end{aligned}$$

$$[0.5 |A_1 A_1 H_2(-j\omega_1, j\omega_1)| + 0.5 |A_2 A_2 H_2(-j\omega_2, j\omega_2)|]$$

Consider the input domain for this system, Fig.2, where 16 points at which the input frequencies intersect correspond to the original 16 complex terms in eqn.(20). These complex terms appear in conjugate pairs to ensure the output $y_2(t)$ is real for the real input. Besides the 4 points on the line $\omega_1 = -\omega_2$ which produce the d.c. response, the other 12 points are pairwise conjugated hence these make 6 significant points. Therefore in total there are only 10 significant points. Furthermore if the transfer function is symmetric, there will be only 6 significant points by the reflectional symmetry about the line $\omega_1 = \omega_2$. They are two zero frequency components or d.c. terms on the line $\omega_1 = -\omega_2$, two harmonics $2\omega_a$ and $2\omega_b$ on $\omega_1 = \omega_2$ and two intermodulations $\omega_a - \omega_b$ and $\omega_a + \omega_b$. If the values at the relevant points of the input frequency intersections are not zero for a given nonlinear system, then nonlinear phenomena will be observed. Hence the same system can have different versions of the transfer function either asymmetric or symmetric but both give the same output. For nonlinear transfer functions there is more than one point which makes a contribution to the final response, even if the input contains only a single frequency. The more frequencies there are in the input the more points will be excited in the input domain.

4. Graphical Representation

The success of the transfer function approach in the linear case can be largely attributed to the simple graphical methods. But for nonlinear systems the main problem of the graphical representation occurs because of the dimensionality. However with the aid of a computer graphics package the second-order transfer function which is most significant for a wide range of nonlinear systems (Vingh et al, 1987) and

the third order transfer function can be plotted. In this section some qualitative analysis is presented in order to improve the understanding of these graphical representations and to show how the analytical results above can be used to aid the interpretation of these plots.

Consider a specific example which is described by the difference equation

$$\text{Example 2: } y(k) = 0.8 y(k-1) + 0.5 u(k-1) + 0.2[\text{NL}] \quad (21)$$

where [NL] is a second order nonlinear term such as $u(k-i)u(k-j)$, $u(k-i)y(k-j)$ or $y(k-i)y(k-j)$ with $i, j = 1, 2, \dots$. The example has deliberately been chosen to have simple dynamics so that the results will be more transparent. Regardless of the form of the nonlinear term, the first order, or linear transfer function is

$$H_1(j\omega) = \frac{0.5 e^{-j\omega}}{1 - 0.8 e^{-j\omega}} \quad (22)$$

Notice that this is the true first order transfer function which will in general be different to the biased estimate obtained from traditional spectral analysis. Fig.3(a) and (b) show the magnitude (in db) and phase of $H_1(\cdot)$, respectively. It is noted that for this discrete time system, ω is the so called normalised or relative frequency. The range $[-0.5, 0.5]$ therefore corresponds to the Nyquist rate for discrete time systems. This can be related to the real frequency provided the sampling frequency is known.

For the second order transfer function $H_2(\cdot)$ it can be shown that the denominator is determined only by the linear output terms so for this specific example the denominator is $[1 - 0.8 e^{-j(\omega_1 + \omega_2)}]$. But the numerator will be dependent on the nonlinear term in eqn.(21). Both the magnitude and phase will be three dimensional plots in terms of ω_1 and ω_2 . Again the magnitude will be displayed in

logarithmic scale using the units decibels. The main advantage of using the logarithmic scale is that the multiplication of magnitudes can be converted into addition and it will be shown below that how this makes the graphical analysis and interpretation much easier. Firstly consider some basic factors which will be encountered in the second order transfer functions. Once the graphical realisation of these familiar factors are made clear in isolation the complete transfer function is easy to understand since it is composed of the addition of individual graphs of these factors:

Numerator Gain K . This is the simplest factor. A number greater than unity has a positive value in db while a number smaller than unity has a negative value. The log-magnitude graph for a constant gain is a horizontal plane at $20 \log K (db)$ (Fig.4). The phase angle of the gain K is zero. The effect of varying the gain K in the transfer function is that it raises or lowers the magnitude of the function by a corresponding constant amount, but it has no effect on the phase angle.

Numerator Phasor $e^{-j(a\omega_1+b\omega_2)}$. This is the fundamental factor or basic building block for discrete-time system transfer functions. Although this term will affect the phase angle, it has no effect on the log-magnitude since its db value is zero. Therefore the magnitude plot is also a horizontal plane, such as Fig.4, but at zero level. However the addition of two distinct phasors has a much more complex graphical realisation. For example

Numerator $e^{-j(\omega_1+3\omega_2)} + e^{-j(3\omega_1+\omega_2)}$. The magnitude of this term is illustrated in Fig.5. Some parallel deep gorges are clearly observed. This is because two exponential phasors cancel occasionally. In this case whenever

$$\omega_1 + 3\omega_2 = 3\omega_1 + \omega_2 \pm (2m+1)\pi \quad m = 0, 1, \dots \quad (23)$$

this can be rearranged to give

$$\Delta\omega = \omega_1 - \omega_2 = \pm \frac{(2m+1)\pi}{2} \quad m = 0, 1, \dots \quad (24)$$

Thus frequencies whose difference conforms to the above cause a gorge. This is confirmed by the contour plot of Fig.5 which is illustrated in Fig.6.

Numerator $H_1(j\omega_1)$ and $H_1(j\omega_2)$. The value of these functions is dependent only on one of two variables and thus the graphical plots Fig.7 and Fig.8 have a simple form in the two-dimensional domain. Any slice cut by $\omega_2 = \text{constant}$ or $\omega_1 = \text{constant}$ is the same as the curve in Fig.3(a). The ridges in Fig.7 and Fig.8 are formed by the dimensional extension which covers the frequency range (-0.5, 0.5).

Numerator $H_1(j\omega_1) + H_1(j\omega_2)$. Fig.9 shows the graph of the addition of these two function. Clearly the algebraic addition is not very evident in the logarithmic plot although some basic characteristics such as two crossed ridges, can still be seen. A distinct new phenomenon is also introduced represented by the presence of two symmetric holes which are located at $(-\frac{\pi}{5}, \frac{\pi}{5})$ and $(\frac{\pi}{5}, -\frac{\pi}{5})$, respectively.

Denominator $\frac{1}{1-0.8e^{-j(\omega_1+\omega_2)}}$. This is only a simple extension of the one dimensional function $\frac{1}{1-0.8e^{-j\omega_1}}$ to two-dimensions (Fig.10). If a sub-domain were introduced with an axis defined as the

summation of ω_1 and ω_2 , i.e., $\omega_{out} = \omega_1 + \omega_2$, the function value would have the same one-dimensional variation along this axis. That is along $\omega_1 = -\omega_2$.

Now consider the whole transfer function corresponding to different nonlinear terms. Consider initially a system with a quadratic nonlinearity in the input of the form $[NL] = u^2(t-1)$ say in eqn.(21). The analytical expression is

$$H_2(j\omega_1, j\omega_2) = \frac{0.2e^{-j(\omega_1 + \omega_2)}}{1 - 0.8e^{-j(\omega_1 + \omega_2)}} \quad (25)$$

which is plotted in Fig.11. Not surprisingly this has the same shape as the denominator plot of Fig.10, because the constant 0.2 only lowers the magnitude while the phasor in the numerator has no effect on the log-magnitude.

For a quadratic output nonlinearity, $[NL] = y^2(k-1)$, the analytical expression becomes

$$H_2(j\omega_1, j\omega_2) = \frac{0.2H_1(j\omega_1) H_1(j\omega_2)e^{-j(\omega_1 + \omega_2)}}{1 - 0.8e^{-j(\omega_1 + \omega_2)}} \quad (26)$$

which is illustrated in Fig.12. Here $H_1(j\omega_1)$ and $H_1(j\omega_2)$ have been imposed and this causes two crossed ridges in addition of the original diagonal ridge. A similar effect is produced by cross-product nonlinearity $[NL] = u(k-1)y(k-1)$ which yields

$$H_2(j\omega_1, j\omega_2) = \frac{0.2[H_1(j\omega_1) + H_1(j\omega_2)]e^{-j(\omega_1 + \omega_2)}}{1 - 0.8e^{-j(\omega_1 + \omega_2)}} \quad (27)$$

This is plotted in Fig.13 and is actually the superposition of Fig.10 and Fig.9.

Up until this point the symmetrisation problem has not been of concern. In the following it will be shown that the symmetrisation can make the graphics much more complicated compared with the asymmetric functions. For a dynamic quadratic input nonlinearity $u(k-1)u(k-3)$, the symmetric second order transfer function is

$$H_2^{sym}(j\omega_1, j\omega_2) = \frac{0.1[e^{-j(\omega_1 + 3\omega_2)} + e^{-j(3\omega_1 + \omega_2)}]}{1 - 0.8e^{-j(\omega_1 + \omega_2)}} \quad (28)$$

The plot of this in Fig.14 is the addition of Fig.5 and Fig.10. The parallel gorges caused typically by the interaction of the two exponential phasors is clear. However the basic asymmetric version is given by

$$H_2(j\omega_1, j\omega_2) = \frac{0.2e^{-j(\omega_1 + 3\omega_2)}}{1 - 0.8e^{-j(\omega_1 + \omega_2)}} \quad (29)$$

or

$$H_2(j\omega_1, j\omega_2) = \frac{0.2e^{-j(3\omega_1 + \omega_2)}}{1 - 0.8e^{-j(\omega_1 + \omega_2)}} \quad (30)$$

which have a much simpler log-magnitude plot similar to Fig.11. It may therefore in some circumstances be more convenient for analysis to use some simple asymmetric versions instead of the traditional symmetrised plots because some of the transfer functions of an equivalent system may have much simpler forms than the others, especially for the higher order cases (Chua and Ng, 1979a; 1979b). Certainly more points need to be considered for an asymmetric transfer function (see section 3).

The above discussion is based on a very simple example with first order dynamics. Needless to say, the approach can be readily applied to higher order cases. For example look at Fig.1(a) the magnitude plot

of example 1 in eqn.(18), this is just the addition of a basic factor(Fig.9) and the second order denominator which is illustrated in Fig.15. Compared to the first order denominator (Fig.10), in Fig.15 there are two ridges about diagonal line. These are caused by the resonance and the two short ridges in the corners are the aliases. Comparatively, in Fig.10 the ridge along the diagonal line results from the symmetry of the graphics, and not the resonance. Fig.16 illustrates that when a *db* scale is used the final form of H_2 is simply the addition of the various components, in this case for the system in example 1.

Finally, it is worth noting that the transfer function representation provides an invariant description of the underlying system irrespective of the form, Volterra or NARMAX, or domain, discrete or continuous. If the model is an adequate description of the system then they will all have exactly the same transfer function. An application of this property is the reconstruction of continuous-time models from sampled-data sets which is based on the observation that these all have the same frequency response function. Many continuous-time examples have also been investigated and it is found that they usually have simpler analytical and graphical representations than the discretised counterparts.

5. Conclusions

From the studies of nonlinear transfer functions it is interesting to find that many results and properties are very similar to and can be considered as simple extensions of the linear case. Both the linear and nonlinear transfer function have two important advantages which are fundamental to most prospective applications. The first is that they convert complex differential/integro operations into simple multiplication/division operations as described above, and the second is that they provide a convenient

way of dealing with the frequency response analysis and interpretation of systems. Furthermore many nonlinear phenomena, which are hidden or disguised in the time-domain description, may easily be revealed and predicted using the nonlinear transfer functions. Since the computation problem has been successfully solved, it is anticipated that the transfer function approach of nonlinear systems analysis will become a very useful tool in many branches of science and engineering.

6. Acknowledgements

The authors gratefully acknowledge the support of Science and Engineering Research Council(SERC) of UK under the contract Ref. GR/F 8564.2.

References

- BILLINGS, S.A. AND TSANG, K.M., (1989). "Spectral Analysis for Nonlinear Systems. Part I - Parametric Nonlinear Spectral Analysis," *J. Mechanical Systems and Signal Processing*, vol. 3, no. 4, pp. 319-339.
- BILLINGS, S.A. AND PEYTON JONES, J.C, (1990). "Mapping Nonlinear Integro-Differential Equations Into the Frequency Domain," *Int J. Control*, vol. 52(4), pp. 863-879.
- CHUA, L.O. AND NG, C.Y., (1979a). "Frequency Domain Analysis of Nonlinear Systems: General Theory," *IEE Journal Electronic Circuits and Systems*, vol. 3, no. 4, pp. 165-185.
- CHUA, L.O. AND NG, C.Y., (1979b). "Frequency Domain Analysis of Nonlinear Systems: Formulation of Transfer Functions," *IEE Journal Electronic Circuits and Systems*, vol. 3, no. 6, pp. 257-269.
- FORNASINI, E. AND MARCHESINI, G, (1978). "Doubly indexed dynamical systems: state-space models and structural properties," *Math. Systems Theory*, vol. 12, pp. 59-72.
- KIM, K.I. AND POWERS, R.J., (1988). "A digital method of modeling quadratically nonlinear systems with a general random input," *IEEE Trans. ASSP.*, vol. ASSP-36, pp. 1758-1769.
- PEYTON JONES, J.C. AND BILLINGS, S.A., (1989). "A Recursive Algorithm for Computing the Frequency Response of a Class of Nonlinear Difference Equation Models," *Int J. Control*, vol. 50, no. 5, pp. 1925-1940.
- TOMLINSON, G.R. AND BILLINGS, S.A., (1991). "Higher order frequency response functions in nonlinear system identification," *Int. Forum on Aeroelasticity and Structural Dynamics*, Aachen, 3-6 June 1991.
- VINH, T., CHOUYCHAI, T., LIU, H., AND DJOUDER, M., (1987). *Second Order Transfer Function: Computation and Physical Interpretation*, 5th IMAC, London.

WIENER, D.D. AND SPINA, J.F., (1980). *Sinusoidal Analysis and Modelling of Weakly Nonlinear Circuits*, Van Nostrand, New York.

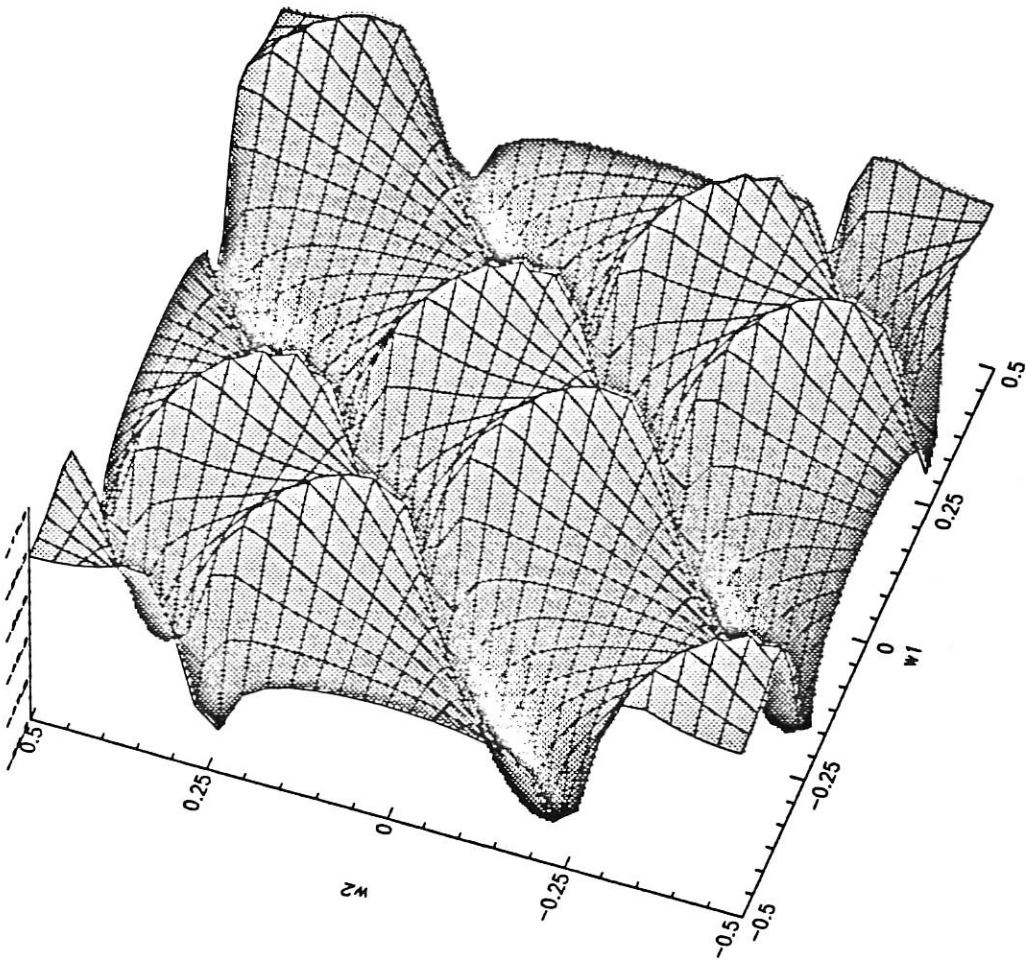


Fig.1(a) Magnitude of $H_2(\cdot)$ of Example 1.

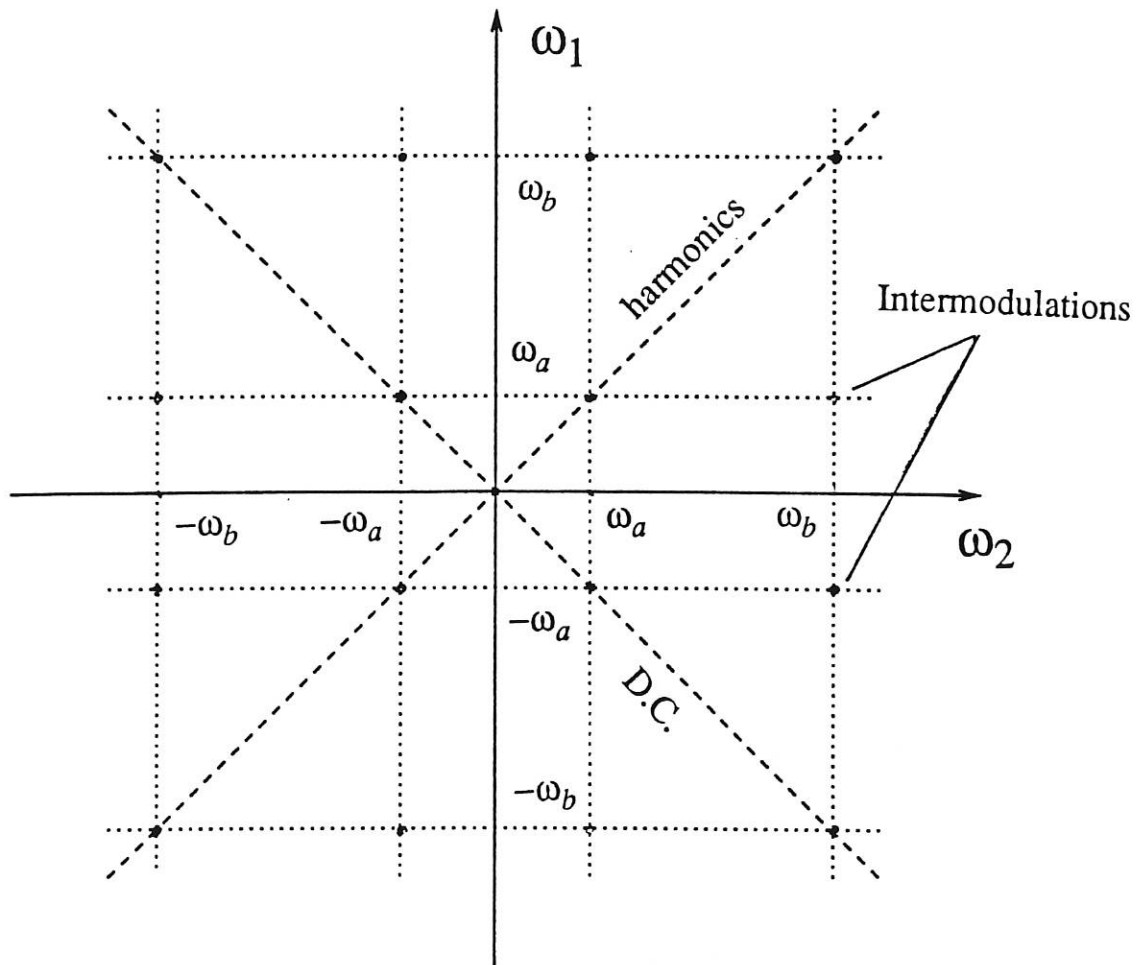


Fig.2 Input frequency domain(for two-tone input).

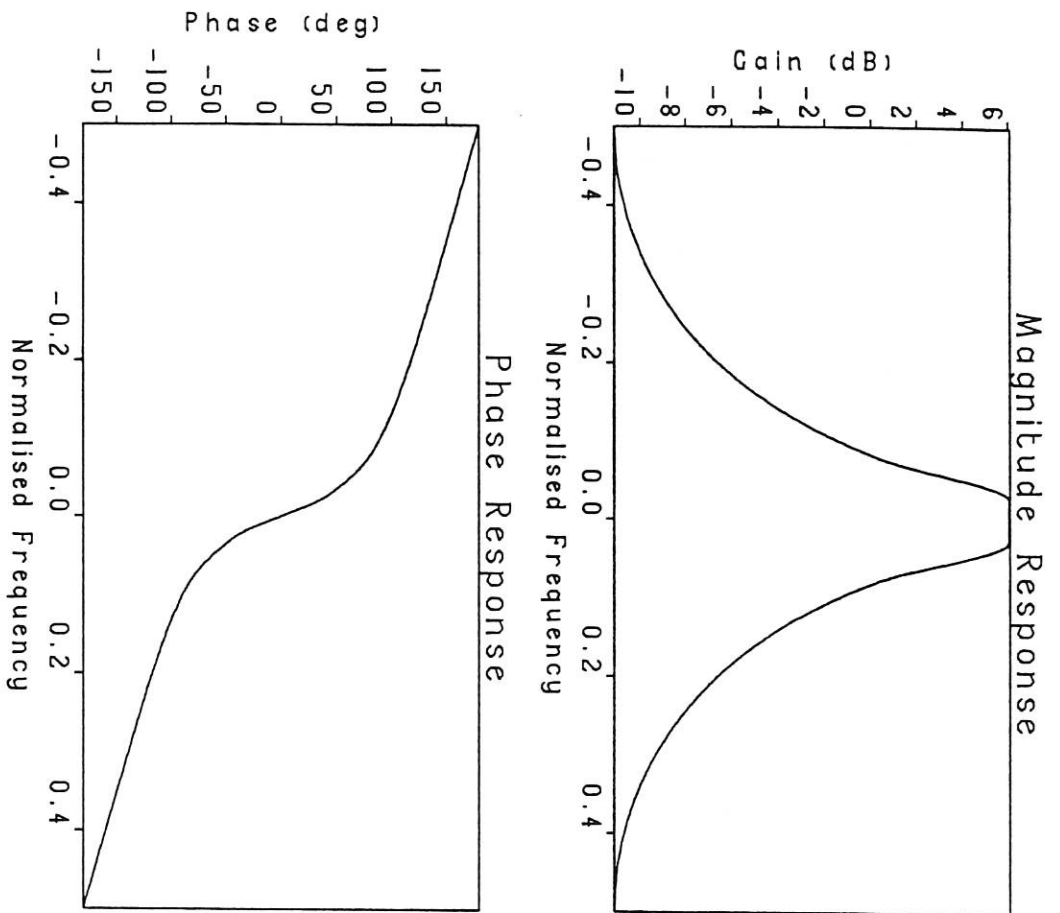


Fig.3 Magnitude and phase of H_1 for Example 2.

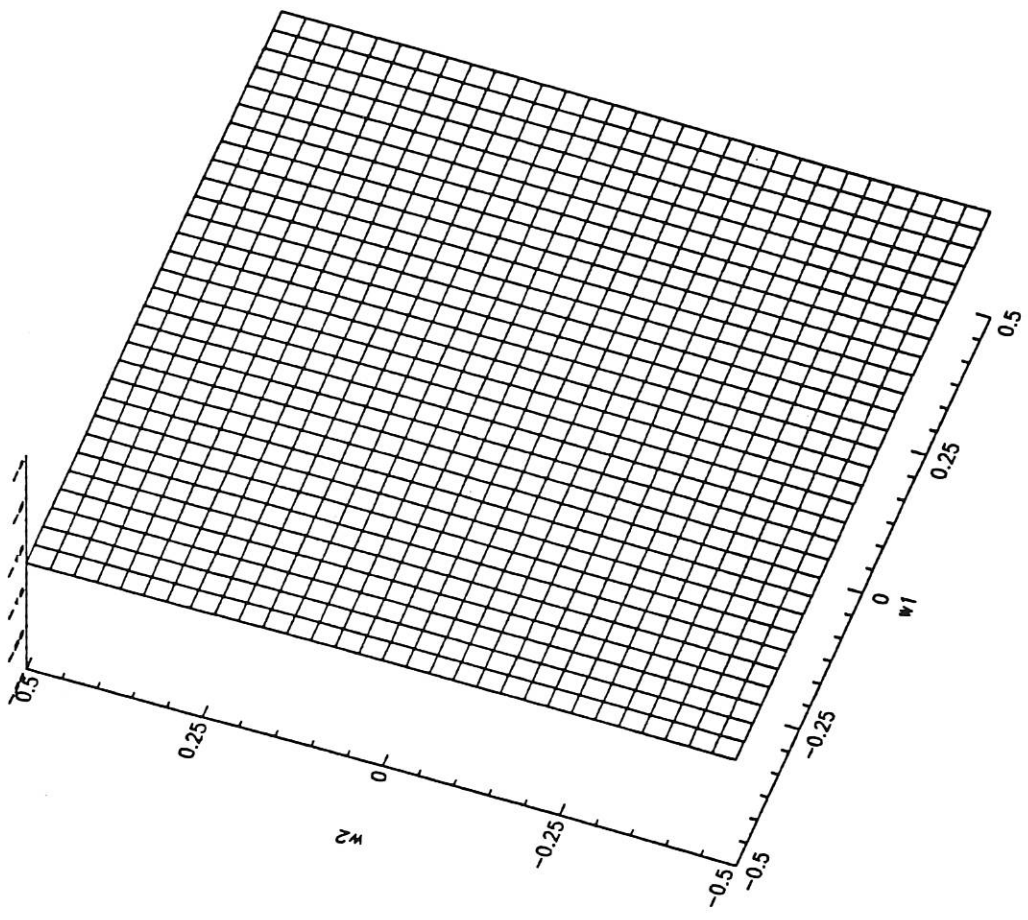


Fig.4 Magnitude for constant factor and single exponential factors.

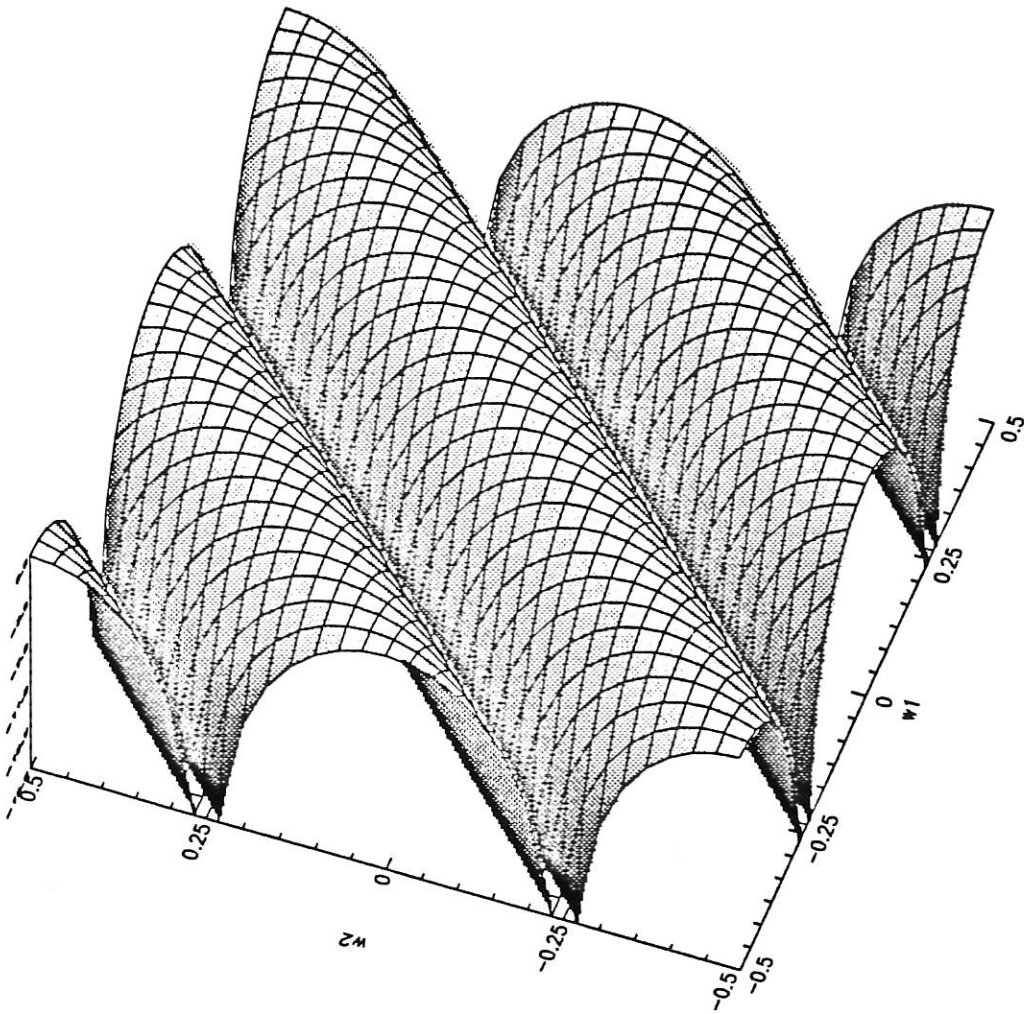


Fig.5 Magnitude for an addition of two distinct phasors.

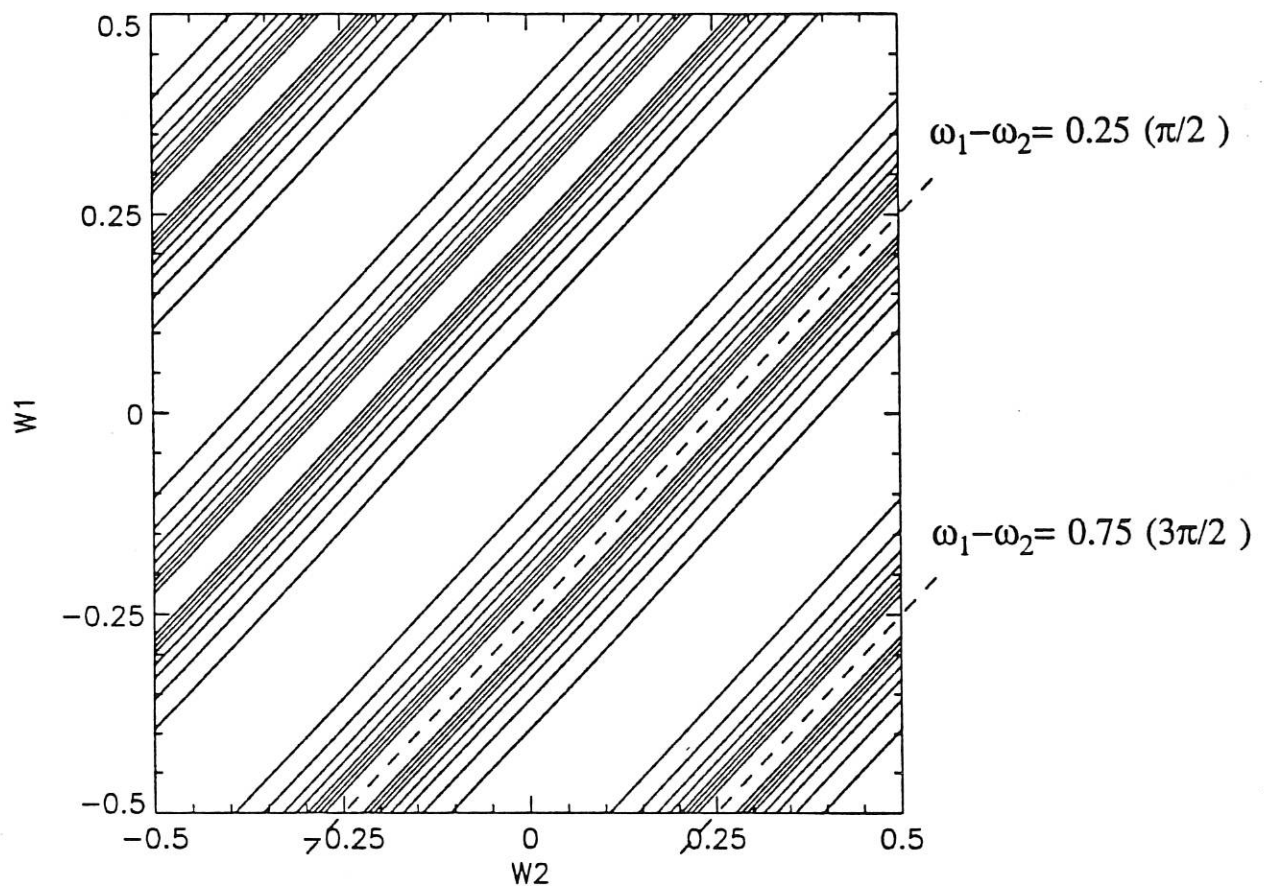


Fig.6 Contour plot of the magnitude for $e^{-j(\omega_1+3\omega_2)} + e^{-j(3\omega_1+\omega_2)}$.

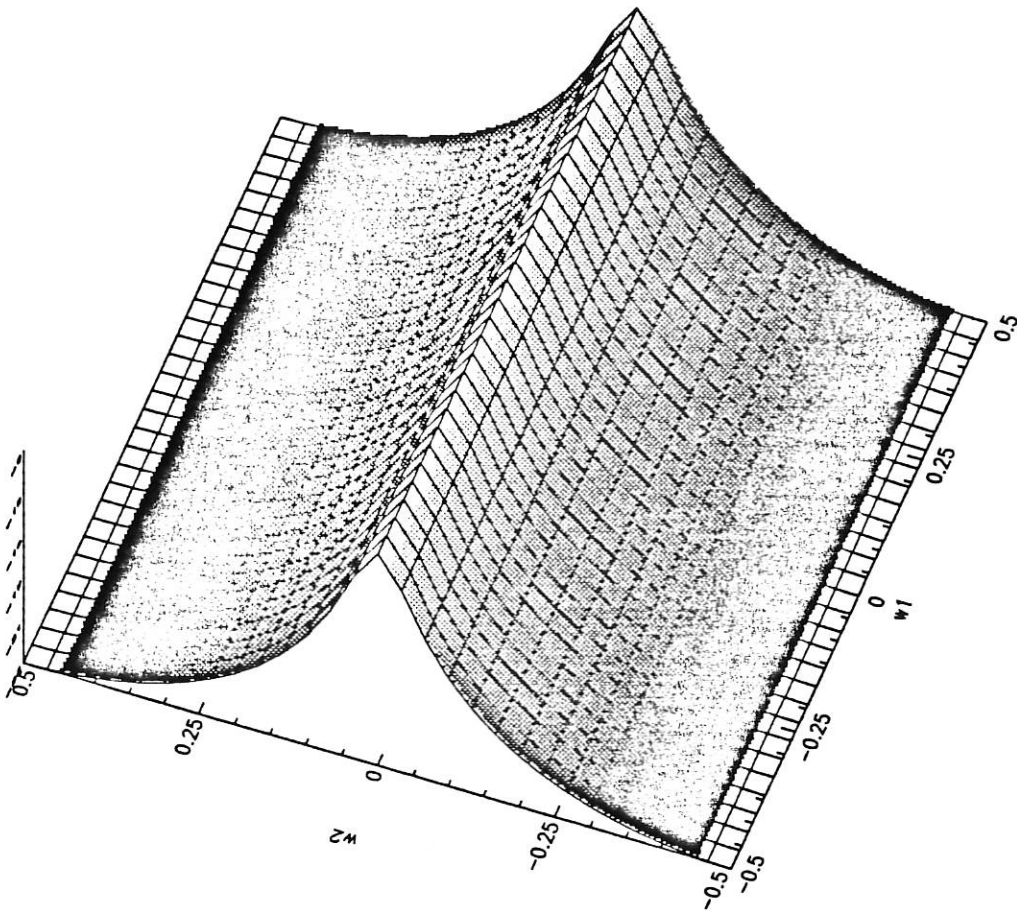


Fig.7 The magnitude of $H_1(j\omega_1)$.

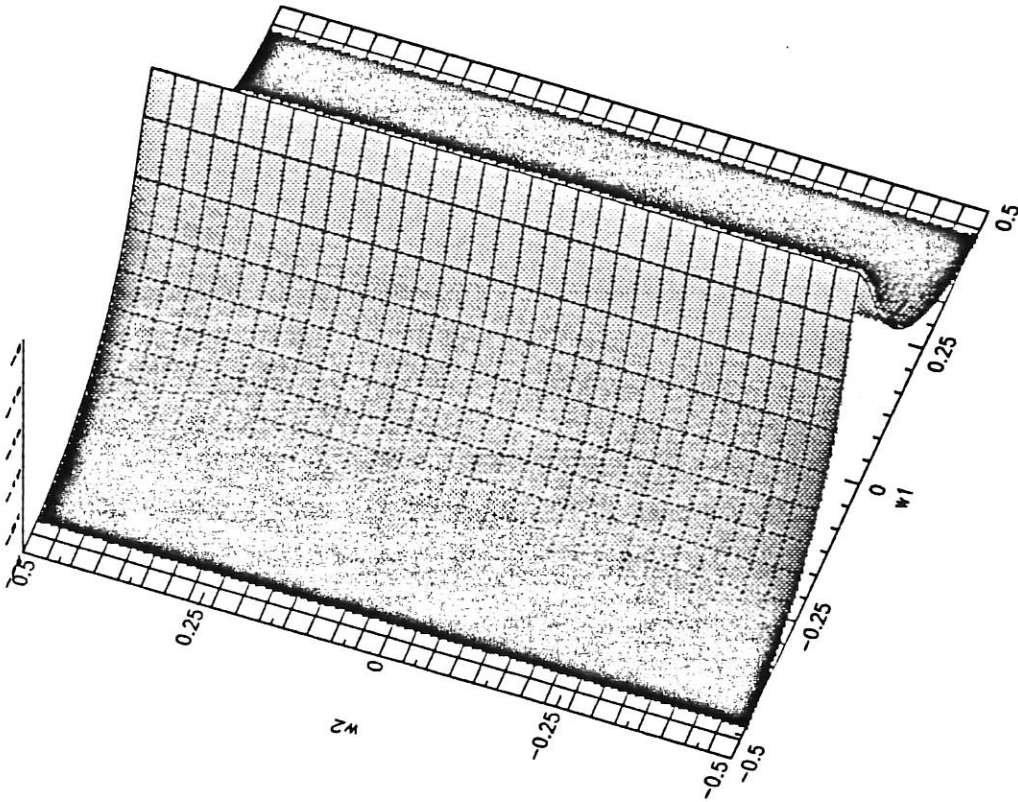


Fig.8 The magnitude of $H_1(j\omega_2)$.

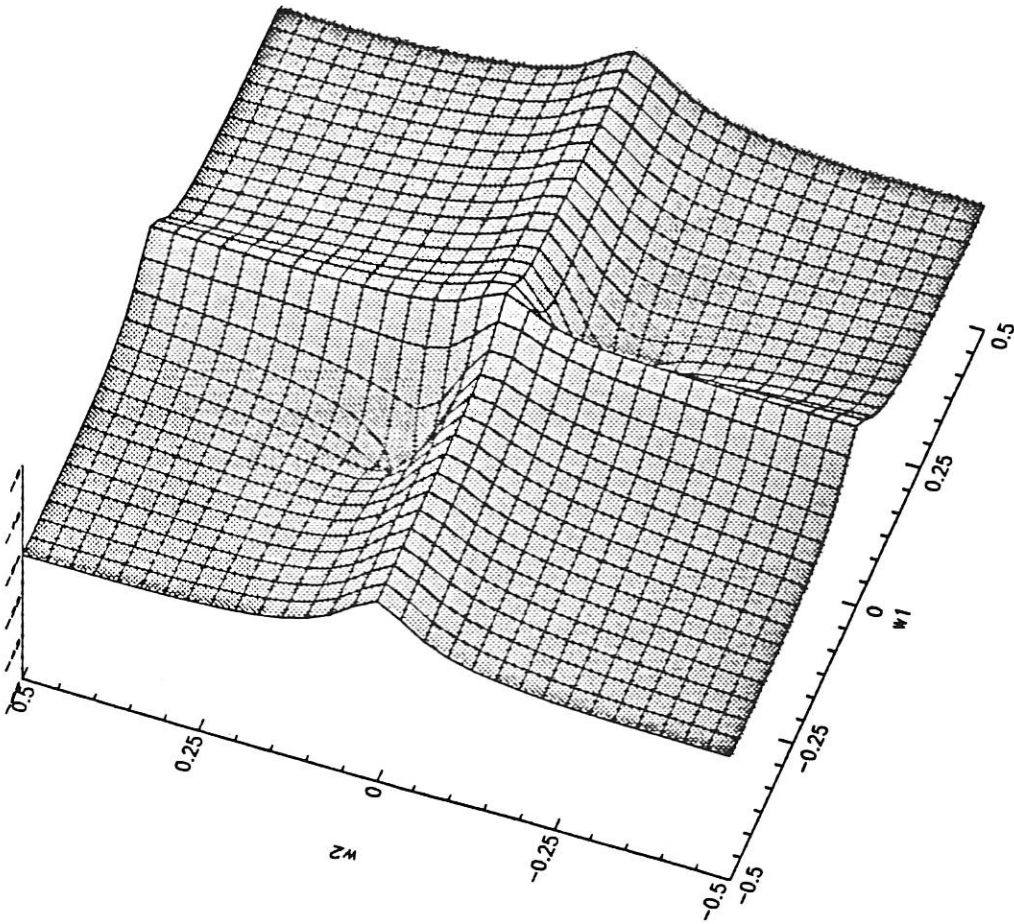


Fig.9 The magnitude of $H_1(j\omega_1) + H_1(j\omega_2)$.

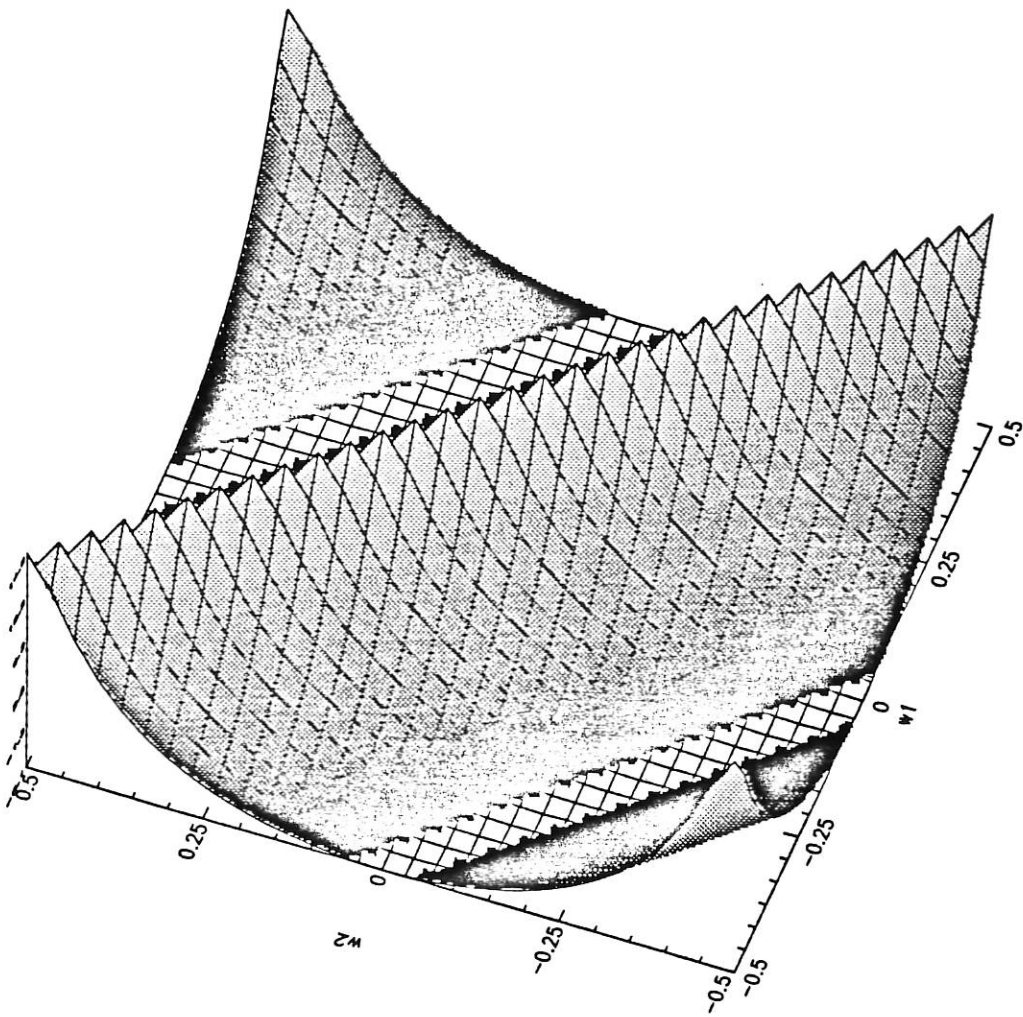


Fig.10 The magnitude of denominator $1/[1-0.8e^{-j(\omega_1 + \omega_2)}]$.

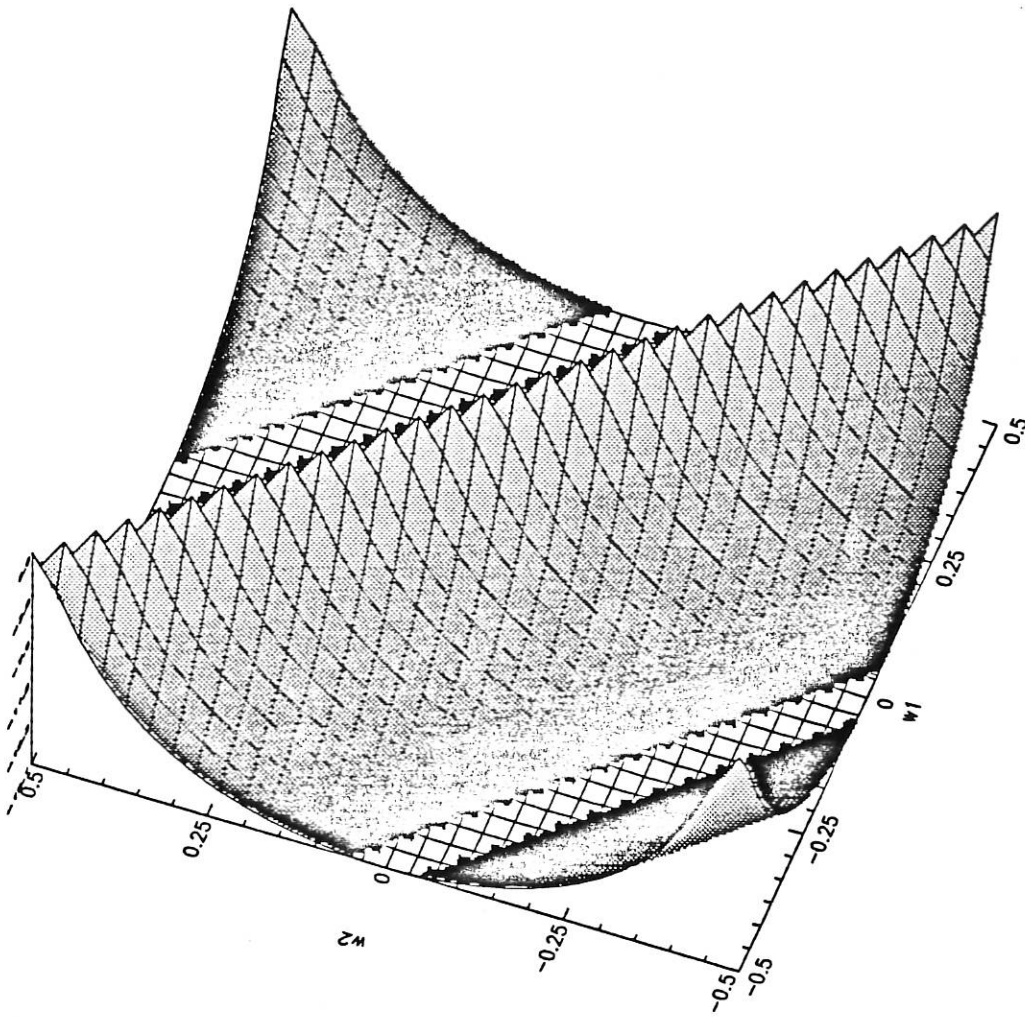


Fig.11 Magnitude of H_2 with nonlinearity $u^2(k-1)$.

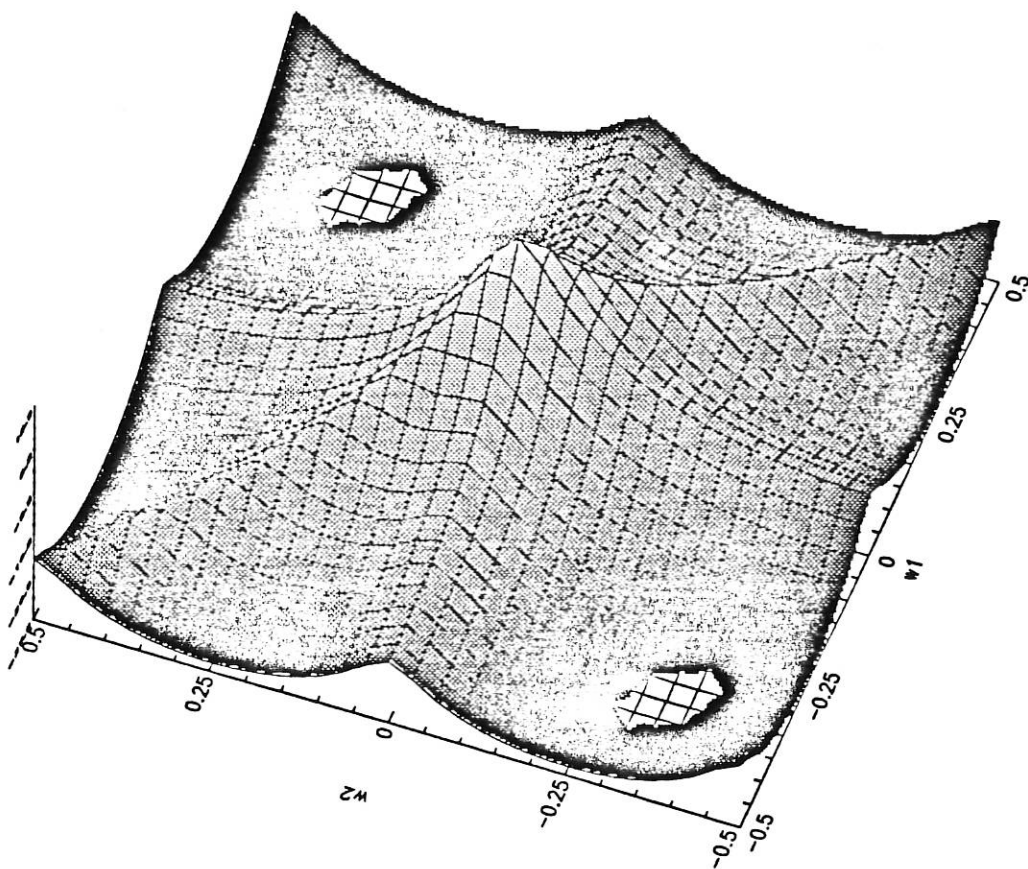


Fig.12 Magnitude of H_2 with nonlinearity $y^2(k-1)$.

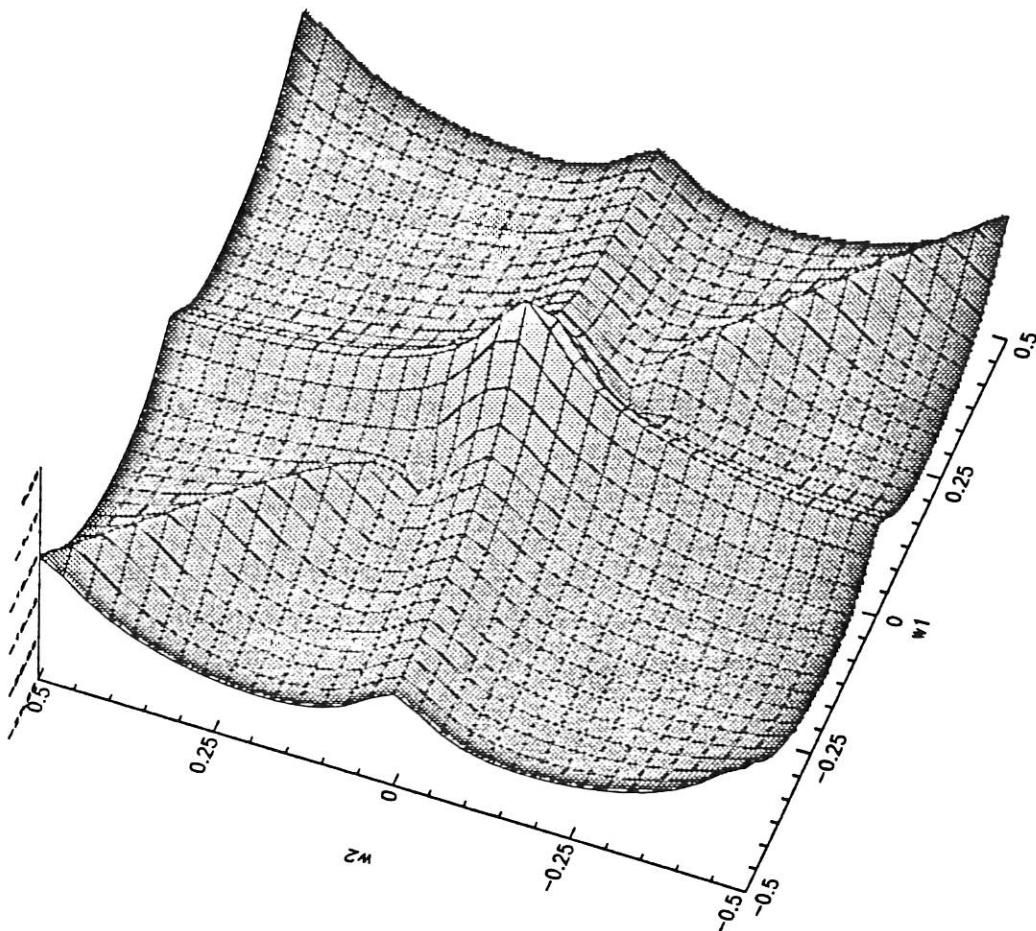


Fig.13 Magnitude of H_2 with nonlinearity $u(k-1)y(k-1)$.

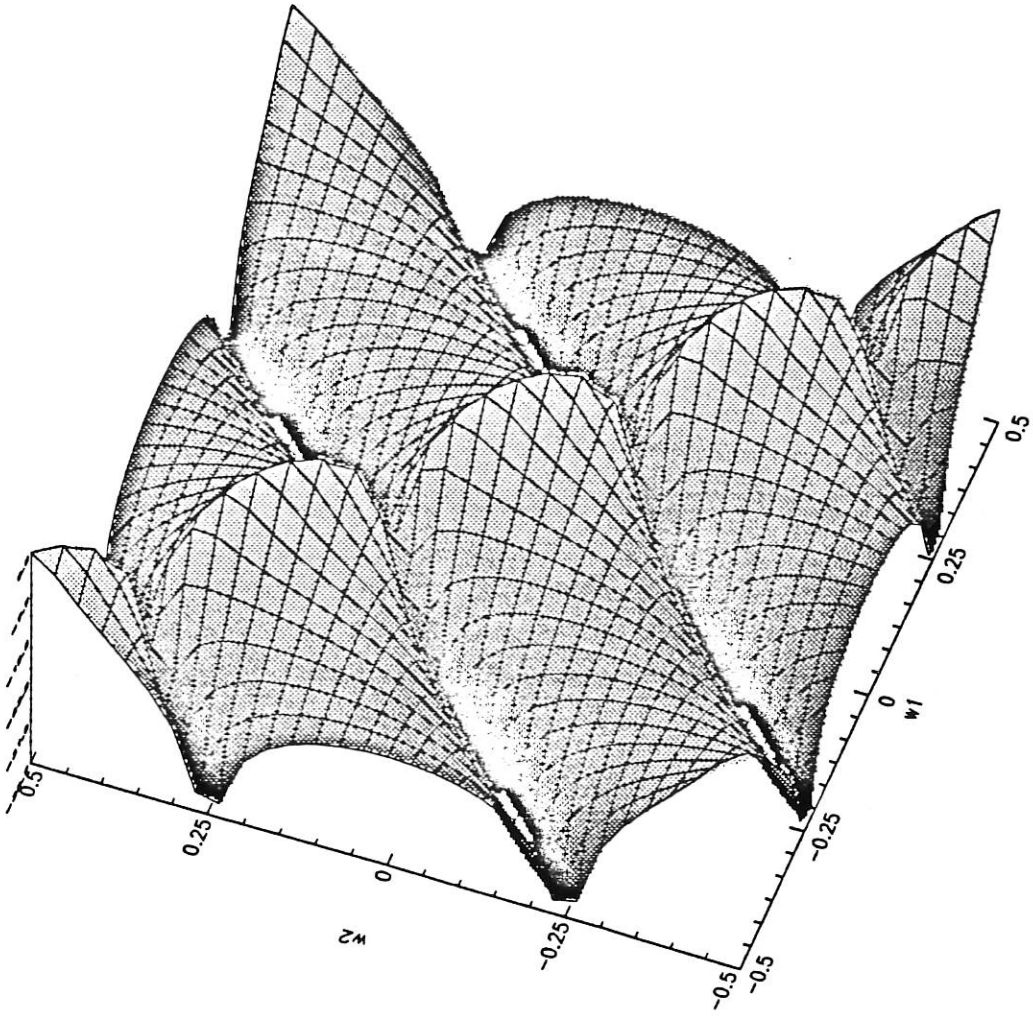


Fig.14 Magnitude of H_2 with nonlinearity $u(k-1)u(k-3)$.

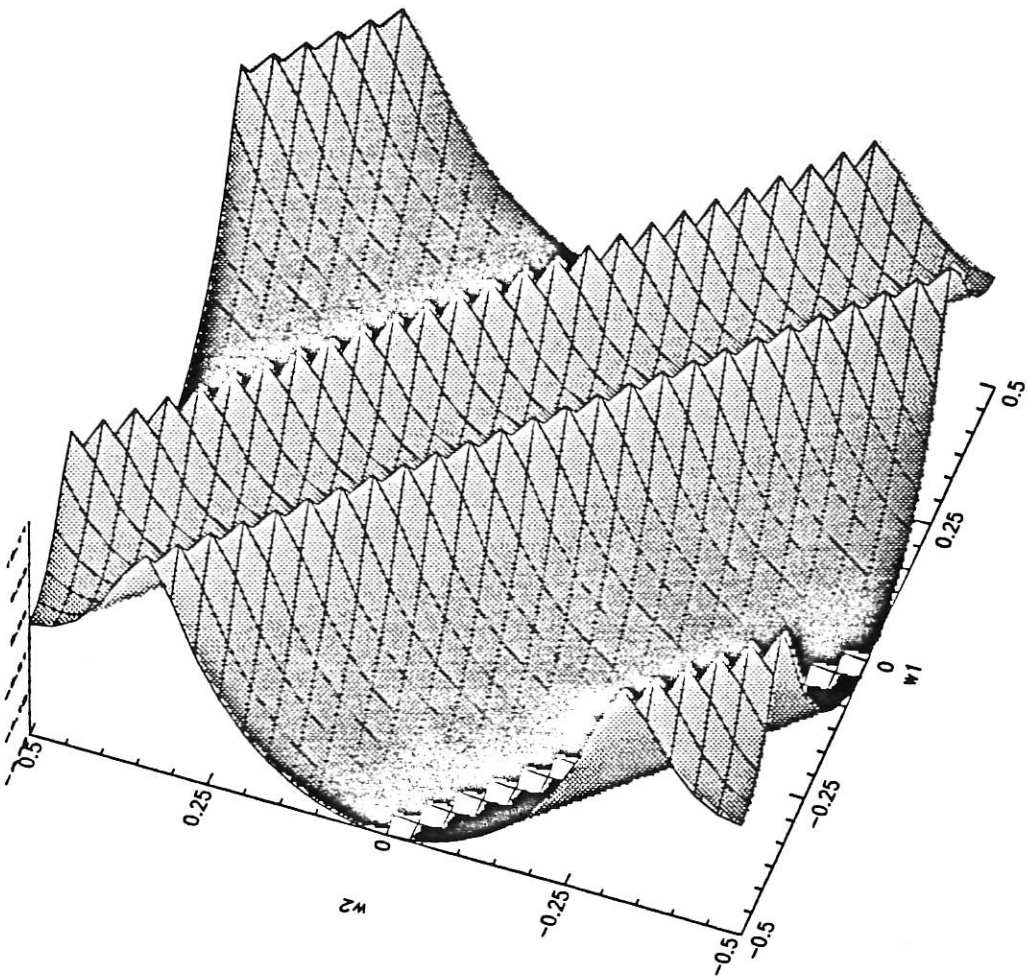


Fig.15 Second order denominator for example 1.

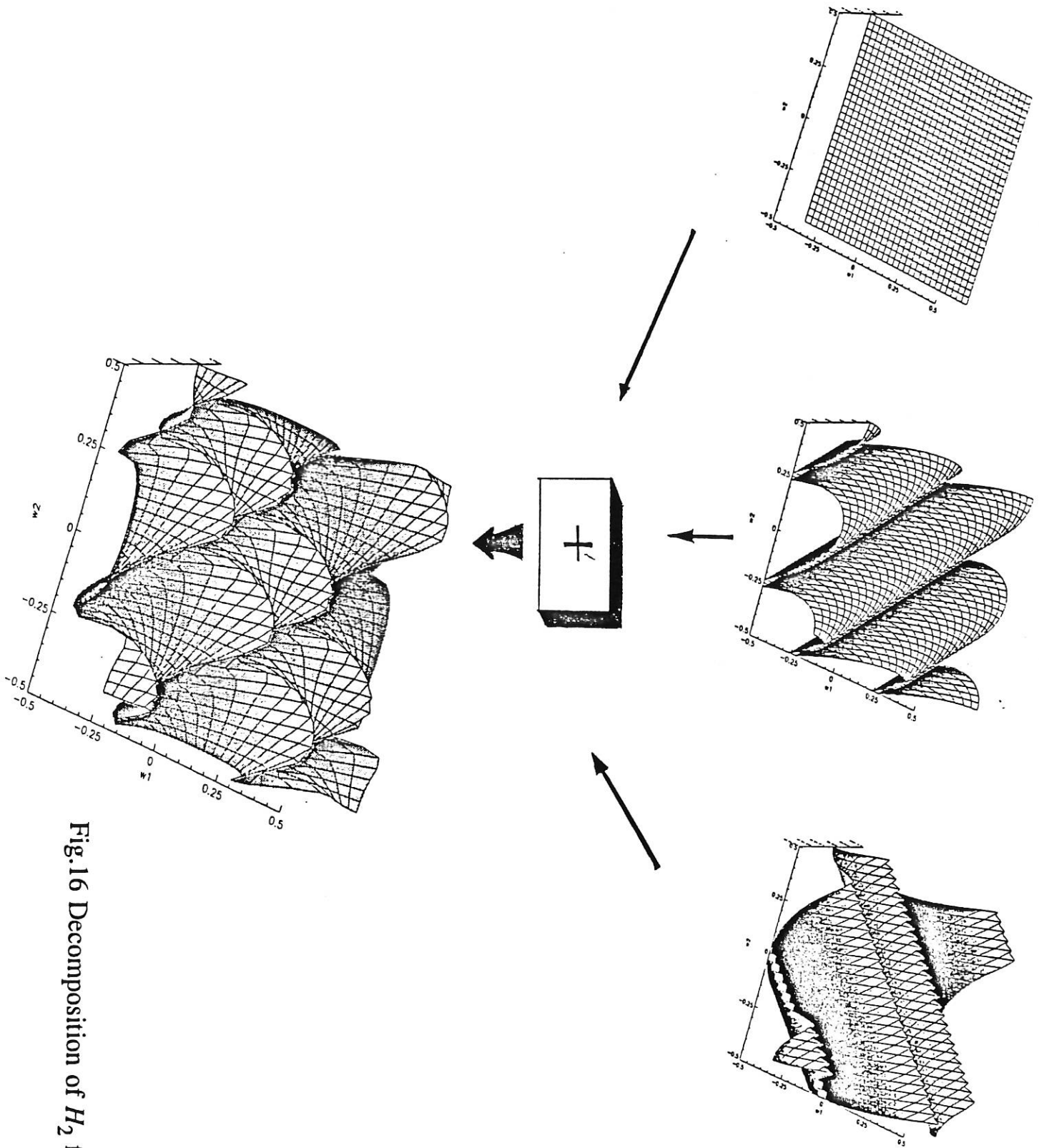


Fig. 16 Decomposition of H_2 for example 1.